CrossMark

ORIGINAL PAPER

Facile synthesis of flexible electrode based on cotton/polypyrrole/multi-walled carbon nanotube composite for supercapacitors

Yang Bo · Yaping Zhao · Zaisheng Cai · Addie Bahi · Caihong Liu · Frank Ko

Abstract Flexible electrodes made of cotton textile, polypyrrole (PPy) and multi-walled carbon nanotubes (MWCNT) composites were synthesized via a facile in situ chemical deposition method. This method involves a series of successive steps by immersing the cotton fabric in various MWCNT suspensions; adding monomers and p-toluene sulfonic acid (TsOH) as dopant under ultrasonic condition; and then initiating the polymerization by drop-in the oxidant. The fabricated electrodes exhibited a specific capacitance of 597 F g^{-1} with good cycle stability (maintaining 96.8% after 1000 cycles). Symmetric all-solid-state supercapacitors based on cotton/PPy/MWCNT electrodes and poly(vinyl alcohol) (PVA)/H_3PO_4 gel electrolytes were fabricated and tested. The electrochemical measurements showed that assembled supercapacitors had a specific capacitance of 206.8 F g^{-1} at a current density of 1 mA cm^{-2}. The supercapacitors were flexible enough to bend and twist with constant capacitance performance and exhibit 72% capacitance retention after 400 charge–discharge cycles.

Y. Bo · Y. Zhao (✉) · C. Liu
College of Chemistry, Chemical Engineering and
Biotechnology, Donghua University, Shanghai 201620,
China
e-mail: zhaoyping@dhu.edu.cn

Y. Zhao · Z. Cai
Key Laboratory of Science and Technology of Eco-
Textile, Donghua University, Ministry of Education,
Shanghai 201620, China

A. Bahi · F. Ko
Department of Materials Engineering, University of
British Columbia, Vancouver, Canada

Springer

Graphical Abstract
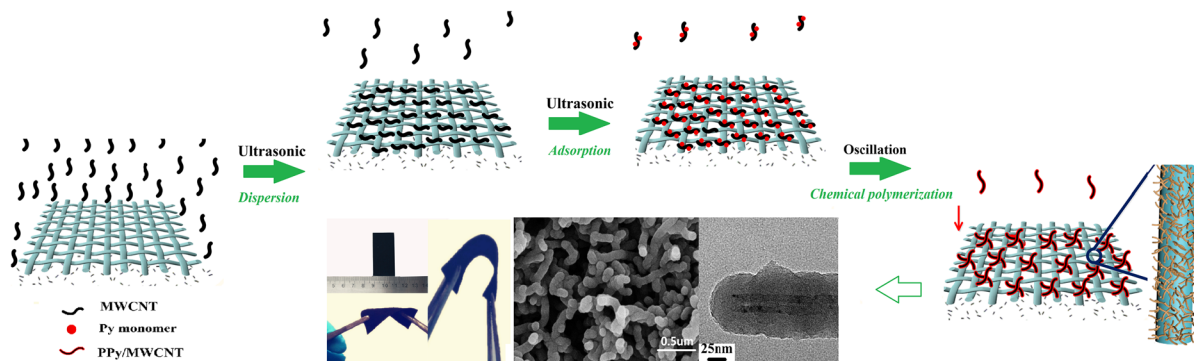
Introduction

Supercapacitors, as a type of high power density capacitor, have drawn considerable attention for their higher power density, longer cycling stability, rapid charging/discharging rate and long-term operation stability (Cai et al. 2015; Huang et al. 2016; Jagadale et al. 2015; Xie et al. 2015; Xiong et al. 2015). Specifically, the fabrication of flexible electrodes for supercapacitors has become emerging field of research (Beidaghi and Gogotsi 2014; Biniak et al. 1995; Xie et al. 2015). In the past decades, a series of related studies have been carried out to rationalize design and synthesis of one-, two-, and three-dimensional conductive materials. Various carbon based materials have been used to prepare conductive papers/textiles including activated carbon, porous carbon, carbon nanotubes (CNTs), grapheme (Li et al. 2013a, 2016; Liu et al. 2010; Wang et al. 2006; Yang et al. 2014), and conducting polymers, such as polypyrrole (PPy) and polyaniline which can be used for supercapacitors (Miller et al. 2011; Nyström et al. 2009; Stoller et al. 2008). However, these materials had some weaknesses, such as poor mechanical stability (swelling, shrinkage, cracks, or breaking), low cycling stability, and limited working potential (Wang et al. 2014).

Numerous investigations have been focused on the new trend of synthesizing composite materials for supercapacitors due to CNTs and conducting polymer composites outstandingly performance (Borenstein et al. 2017; Gao 2017; Lee et al. 2014; Song et al. 2016). Among various conducting polymers, PPy is of particular interest due to its environmental stability, high conductivity, good redox properties, reasonable commercial availability of initial monomers, and simple synthesizing procedures. It is believed that adding carbon nanomaterials, e.g. graphene and CNT, can significantly enhance capacitive stability and charge storage capability of the resultant PPy nanocomposite owing to the improvement of the ion diffusion rate and increasing the contact surface area (Qian et al. 2013; Sawangphruk et al. 2013; Tang et al. 2015).

Recently, considerable effort has been devoted to producing PPy/CNT composites via in situ chemical polymerization (Karim et al. 2007; Shi and Zhitomirsky 2013; Zhang et al. 2011). The fabrication of PPy/CNT composites on insulate substrates is usually carried out by two-steps: the substrates are coated with CNT by various methods, and then chemical or electrochemical deposition applied to growing the polymers on the surface of CNT (Kim et al. 2008; Liu et al. 2015; Yesi et al. 2016); or the PPy/CNT composites are first prepared and then they were applied on the substrates (Li et al. 2013b). Huang et al. used electrochemical method synthesized cotton/PPy/CNT/electrode by two steps: the first step was prepared a cotton/CNT conductive substrate and the second step was by electropolymerazation of PPy on cotton/CNT substrate (Huang et al. 2016). Our group has reported the cotton/PPy/MWCNT electrode which was synthesized electrochemically by the same two steps (Liu et al. 2016). Compared with the electrochemical method, considering the limitations in terms

of mass production, the chemical method gives a higher yield, provides a simpler operation route and involves inexpensive agents, such as $FeCl_3$ and ammonium persulfate, which consequently are preferred for mass-production in industry (Kang et al. 1991; Xu et al. 2015a, b, c). Thus, one-pot chemical deposition of PPy/CNT composites on substrate through cotton fabric immersed in MWCNT suspention and then added py monomers which were oxidant to PPy by $FeCl_3$, will be an alternative route for application in industrial production due to its convenience and efficiency.

Within various methods for fabricating high-performance electrode, the convenient and efficient path of coating or growing active materials electrochemically on lightweight flexible substrates, such as paper, textile has attracted considerable attention (Ge et al. 2015; Hu and Cui 2012; Hu et al. 2010; Liu et al. 2014; Wang et al. 2013). Among the candidate substrates, cotton fabrics have an ideal skeleton to construct complex and multifunctional layers considering their intrinsic porosity, toughness and natural abundance (Bao and Li 2012; Liu et al. 2012; Xue et al. 2013). In this study, cotton/PPy/MWCNT composite electrodes were synthesized through a facile one-pot chemical method. The as-prepared cotton/PPy/MWCNT composite electrodes presented in the 3D porous structures were evaluated. Electrochemical performances of the flexible supercapacitors made of cotton/PPy/MWCNT, as electrodes, and PVA/H_3PO_4, as gel electrolyte, were tested on electrochemical station in two-electrode supercapacitor testing cells.

Experimental

Materials

0.4 mm thick cotton fabrics (with areal density of 277.0 ± 2.0 g m^{-2}) were provided by Jiangsu Dayao textiles Co. Ltd. in China. The multi-walled carbon nanotubes (MWCNT) were purchased from Nanotech Port Co, Ltd. (Shenzhen, China). Pyrrole was purchased from Sinopharm Chemical Reagent Co., and purified through distillation under reduced pressure before use. All other reagents were of analytical reagent grade, purchased from Sinopharm Chemical Reagent Co., Ltd., and used without any further

purification. All aqueous solutions were prepared with deionized (DI) water.

Preparation of cotton/PPy/MWCNT electrode

The cotton fabric was treated with 10 g L^{-1} aqueous sodium hydroxide (NaOH) at 95 °C for 1 h to remove the residual impurities. MWCNT was treated by refluxing in nitric acid (HNO_3) at 110 °C for 4 h (the MWCNT used below are all acidified).

The cotton fabric was immersed in MWCNT/sodium dodecylbenzenesulfonate (SDBS) suspension, which was prepared via dispersion/sonication at room temperature for 1 h, the ratio of fabric mass (g) to liquid volume (ml) was 1:40. Then, 0.5 M Py and TsOH were added into the solution and it was sonicated for another 0.5 h. Finally, the reaction solution was transferred to the Water-bathing Constant Temperature Vibrator, and 0.75 M $FeCl_3$ aqueous solution was added drop by drop into the reaction solution slowly under 0 °C and oscillation for 2 h, the volume ratio of $FeCl_3$ aqueous solution to monomer suspension was 1:10. After polymerization, the composite fabrics were soaked in ethanol for 10 min, 1 M HCl for 30 min, and then washed with DI water several times, dried in a vacuum oven at 40 °C for 24 h.

Fabrication of all-solid supercapacitor

A mixture of PVA powder (6 g), H_3PO_4 (6 g), and DI water (60 ml) was heated to 85 °C with stirring for 2 h to prepare PVA/H_3PO_4 gel electrolyte. Then two identical electrodes, as described above (1 cm × 2 cm), were immersed into PVA/H_3PO_4 gel electrolyte for 6 h. This was followed by placing a non-woven separator in between the two electrodes and dried at room temperature for 6 h resulting in an all-solid supercapacitor. This device was flexible capable of bending and twisting without delamination.

Characterization

The morphology of the samples was studied by field-emission scanning electron microscope (FESEM; Hitachi S-4800, Japan) and a transmission electron microscope (TEM, JEM-2100, JEOL). Energy dispersive spectrometer (EDS, Bruker Quantax400, and Germany) was used to examine the content of PPy and

MWCNT in the composite electrode. The structure of the electrodes was studied by X-ray diffraction (D/max-2550VB+/PC). All the electrochemical measurements were performed on an electrochemical workstation (CHI 660E, Shanghai Chenhua Instrumentco., LTD China). The electrochemical performances of as-prepared samples were tested based on a three-electrode cell in 2 M NaCl aqueous electrolytes; the cyclic voltammetry (CV), and galvanostatic charge–discharge were carried out from 0 to 0.8 V; the EIS tests were carried out in the frequency range from 0.01 Hz to 100 kHz. The electrochemical performance of the fabricated supercapacitors was tested in a two-electrode cell system.

Results and discussion

The formation mechanism of cotton/PPy/MWCNT electrode

Figure 1 shows a schematic illustration of the preparation of the PPy/MWCNT composite layers on cotton fabric based on a one-pot in situ chemical oxidation polymerization method. In order to improve the synthesis process, the following four points should be taken into consideration:

(1) Homogeneous dispersion of MWCNT in the aqueous reaction system is one of the key points for uniform coating of PPy/MWCNT on the surface of cotton fabric. Because of its hydrophobic nature and strong van der Waals interactions, MWCNT precipitate easily into the yarns or bundles in aqueous solutions (Shi and Zhitomirsky 2013). By adding a surfactant, such as SDBS, charged SDBS molecules showed strong adsorption towards the surface of the MWCNT due to the π–π interactions and provided electrostatic dispersion (Tamm et al. 2007; Wang and Yu 2012).

(2) The hydroxyl and carboxyl active groups on acid-treated MWCNT likely provide a binding force between MWCNT and cotton fabric (which consists mostly of hydroxyl groups on cellulose fibers). Also these groups provide the interfacial interaction between MWCNT and PPy due to the hydrogen bonds formed between –COOH groups of chemically modified MWCNT and N–H groups of the PPy (Zhang et al. 2011).

(3) TsOH, as a dopant, plays an important role in the production of PPy with high-performance, since PPy with larger-sized dopant anions (p-toluenesulfonic anion, TsO$^-$) exhibits better ion exchange ability than those doped with smaller inorganic anions, such as Cl$^-$ and NO$_3^-$. Otherwise, the hydrophilic sulfonate groups of TsOH were negatively charged and were absorbed by the cationic pyrrole radicals produced during the polymerization of PPy.

(4) The adding sequence of MWCNT, monomer, initiator, and substrate is critically important for providing an in situ chemical polymerization on
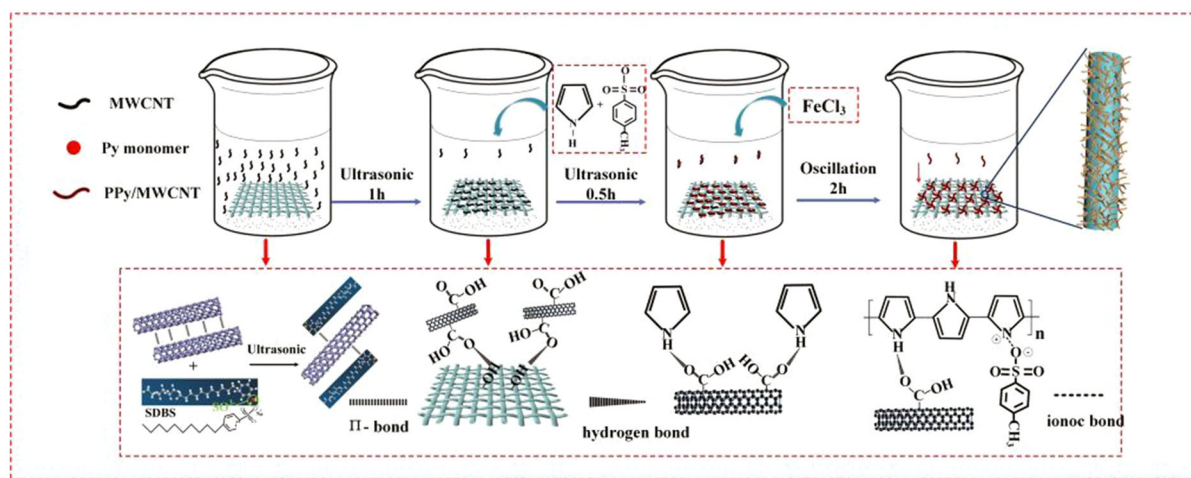

Fig. 1 A schematic of the preparation of the cotton/PPy/MWCNT electrodes

the surface of substrates. The first pre-deposition step of carbon nanotubes on cotton fabrics and then addition of monomer and dopant under ultra-sonication facilitated the nucleation of PPy on MWCNT instead of the cotton fibers. Moreover, ultrasound was applied to achieve a

better dispersion of MWCNT and pyrrole in aqueous solution and the ultrasound bath was used to prevent the nanoparticles from aggregating and penetrating into the fibers of the fabric before chemical polymerization.
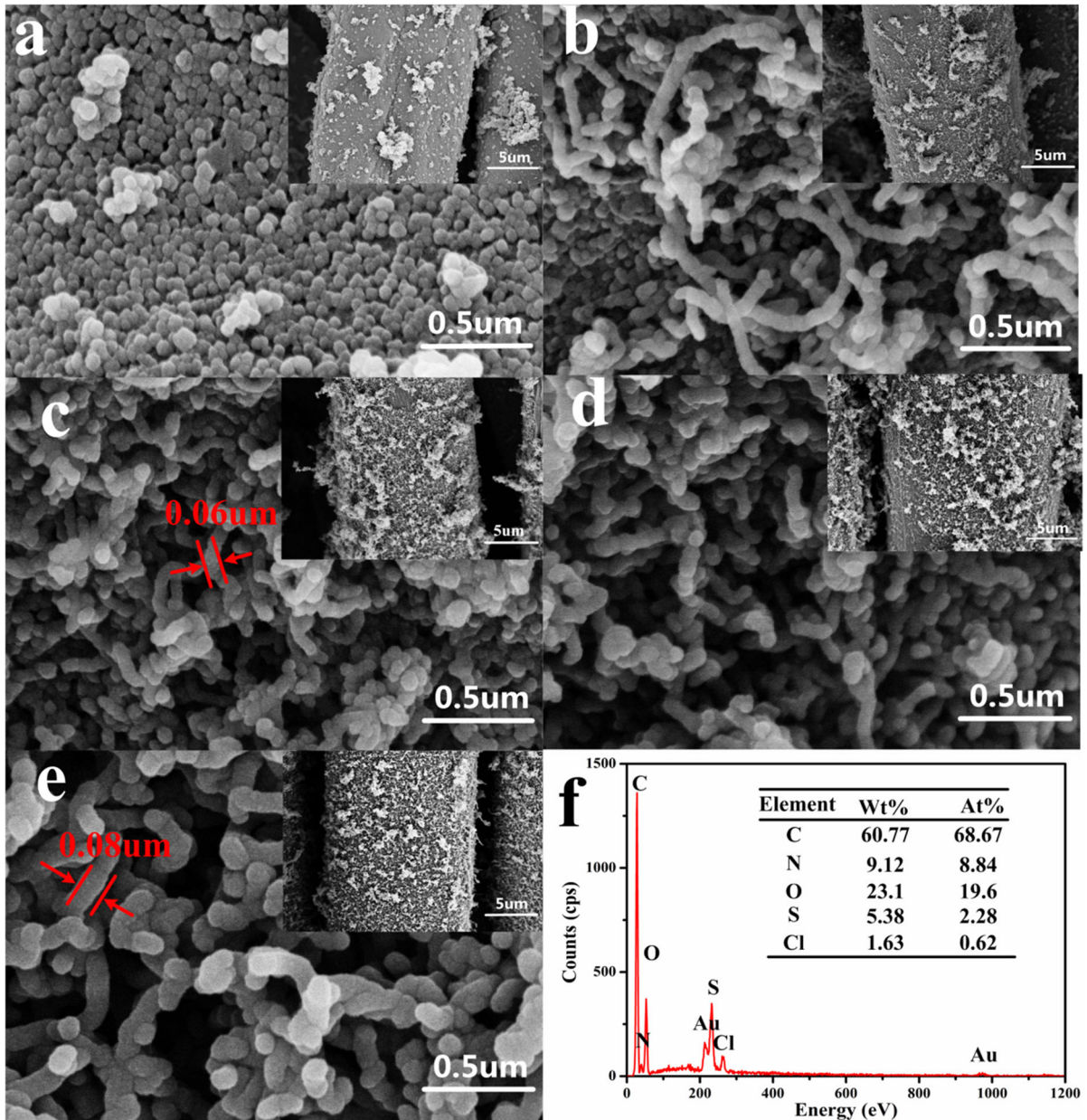

Fig. 2 FESEM images of the electrodes prepared with different MWCNT content under 0.05M TsOH: **a** MWCNT–PPy(0%)-L, **b** MWCNT–PPy(10%)-L, **c** MWCNT–PPy(20%)-L, **d** MWCNT–PPy(30%)-L, **e** The FESEM image of the

MWCNT–PPy(20%) prepared under 0.15 M TsOH, **f** EDS spectra and the surface element content of the cotton/PPy/MWCNT electrode

The morphology and structure of cotton/PPy/ MWCNT electrode

Figure 2a shows PPy particles with spherical morphology on the surface of cotton fibers when no MWCNT were added. It was noted (Fig. 2b–d) that MWCNT–PPy sediments (the PPy wrapped the MWCNT surface in a regular manner using each MWCNT bundle) increase with increasing mass ratio of MWCNT to pyrrole. Compared with cotton fibers, the larger surface area of MWCNT coated in cotton, the higher surface activity in electrode reaction. When the mass ratio of MWCNT to pyrrole was less than 20%, a higher density of nanocomposites with the tube diameter estimated to 60–70 nm in a three-dimensional structure involving PPy growth along with MWCNT, can effectively increase the contact area between the electrode materials and electrolyte. The diameter of MWCNT–PPy(20%) prepared under 0.15 M TsOH increased to 80–90 nm (Fig. 2e), compared with the MWCNT–PPy(20%)-L under 0.05 M TsOH (Fig. 2c). In addition, it was observed that the external surface of nanotubes of MWCNT–PPy(20%) were less smooth than that of MWCNT–PPy(20%)-L, which indicates that TsOH favors the PPy coating and thus leads to a relatively thicker layer of coating on the MWCNT surface.

Cotton fabric has many advantages over other platforms in the development of flexible electrode, such as large surface area and a natural 3D mesh structure. The FESEM image (Fig. 2e) shows that the cotton fiber was coated by MWCNT–PPy composite materials uniformly and the PPy coating grew along the MWCNT, resulting in a uniform 3D mesh composite structure. The 3D porous structure increases the contact area between the electrode materials and electrolyte, and at the same time, the electrolyte ion transport rate and the reaction of the electrode material were improved significantly. Additionally, the cycle stability of the composite material is benefit from the special 3D structure. The formation of MWCNT–PPy coating in MWCNT–PPy(20%) was further proved using EDS spectra (Fig. 2f). The elemental analysis of the atomic concentrations was: carbon (68.67%), nitrogen (8.84%), oxygen (19.60%), sodium (2.28%), and sulfur (0.62%). The PPy layer, as a source of nitrogen, was detected and the presence of sodium confirms the doping of TsO^- and $SDBS^-$ in chemical polymerization. In addition, chlorine

Fig. 3 a–c Different magnification TEM images of MWCNT–▶ PPy(20%) composites, d digital photographs of the flexible PPy/ MWCNT/cotton fabric electrodes, e XRD pattern of pure cotton fabric and those MWCNT–PPy composite-based cotton fabrics

appeared in the spectra, because the oxidant $FeCl_3$ contains large amounts of Cl^-.

A TEM image of MWCNT–PPy(20%) composites is shown in Fig. 3. The surface of MWCNT–PPy(20%) composite appears to be smooth and uniform, and there are no agglomerations or irregular nanoparticles of polymer after ultrasonic dispersion (Fig. 3a, b). The image reveals a coaxial structure of the resulted MWCNT–PPy composites in which the MWCNT is encapsulated by a uniform shell of PPy. Figure 3c shows a high-resolution TEM image of a segment of MWCNT coated with the polymer shell. The original MWCNT core with a crystalline lattice structure and an amorphous PPy coating layer can be clearly identified. Compared with the MWCNT, the diameter of MWCNT–PPy(20%) nanotubes increased from 30–40 to 80–90 nm, and their external surface were less smooth.

Figure 3e depicts the XRD pattern of pure cotton fabric, and MWCNT–PPy composite-based cotton fabrics. The diffraction peaks of the pristine cotton fabric are showed as: (101) at $2\theta = 14.7°$, (101) at $2\theta = 16.6°$, (021) at $2\theta = 20.6°$, (002) at $2\theta = 22.7°$, (040) at $2\theta = 34.7°$, which correspond to the crystalline structure of cellulose (Firoz et al. 2013; Ford et al. 2010). After coating the cotton fabric with PPy or MWCNT–PPy, the crystalline nature of all the cotton fabrics remains the same. The plane (002) was affected during the modification and the relative intensity of this plane was reduced accordingly. The peak at $2\theta = 22.7°$ for cotton was observed at the same position for MWCNT–PPy(10%) and was shifted to $2\theta = 22.9°$ for cotton/PPy, cotton/MWCNT–PPy(20%) and cotton/MWCNT–PPy(30%) related to the crystalline structure of the samples. For the different mass ratio of MWCNT–PPy, the XRD spectra showed that the MWCNT peak at 26.2° corresponding to the (002) reflections of the carbon atoms. It is clear that the peak intensity increased with the increase of the mass ratio of MWNTs to pyrrole.
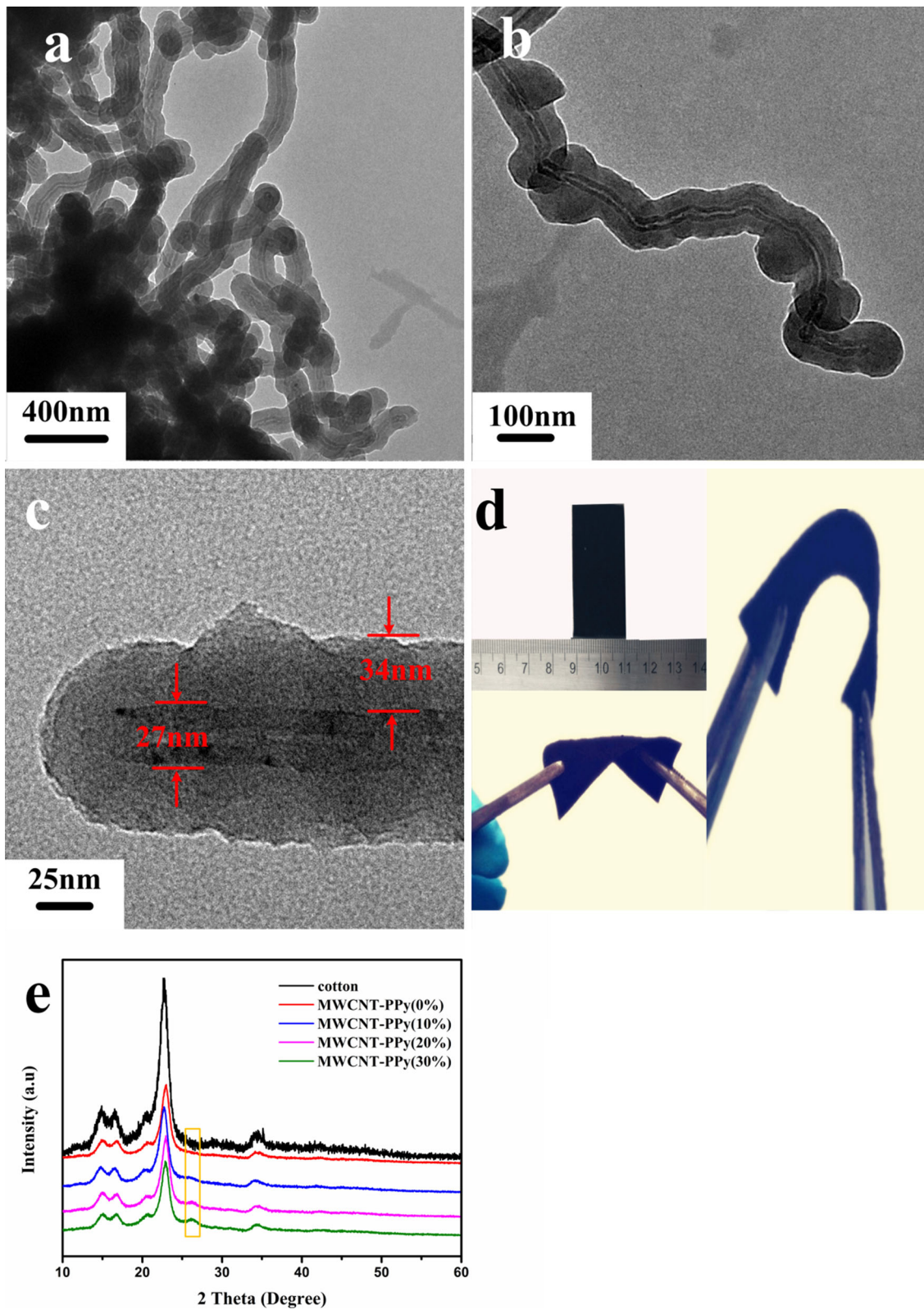
The electrochemical of cotton/PPy/MWCNT electrode

The influence of MWCNT on the sheet resistances of the composites can be seen in Fig. 4a showing that the PPy–MWCNT(20%) composites exhibited the highest conductivity compared to other composites. The capacitance retention (Fig. 4b) showed that the increase in MWCNT content in the composites resulted in high stability of capacitance due to the inherent cycle stability of carbon materials. Figure 4c–e presents the electrochemical test for the synthesized electrodes. As shown in Fig. 4c, when the scan rate is lower, there is obvious redox peak, but the redox peak decreased with the increase of scan rate. These results show that the redox reaction of the electrodes can react completely with enough time under low scan rate. The high specific capacitance (597 F g^{-1}) can be calculated using the CV curves at a scan rate of 1 mV s^{-1}. GCD curve also confirms the high capacitance of the electrode shown in Fig. 4d. The cycling stability of the electrode was tested by CV curves at a scan rate of 100 mV s^{-1} (Fig. 4e). The high capacitance retention of the electrode (96.8%) benefited from the added MWCNT and the three-dimensional structure of the cotton fabric. The smaller the diameter of the semicircle area in the high-frequency portion of the plot is, the higher the ion diffusion of the electrode will be. Figure 4f confirms a smaller diameter (the inset) of the semicircle indicating the good property of the electrode.

The performance of supercapacitor

In order to assess the performance of the composite device, a series of symmetric supercapacitors were fabricated using the electrodes mentioned above (Fig. 5a). The mass specific capacitance (C$_m$, F g^{-1}) from the charge–discharge curves was calculated according to the following integral Eq. (1). The energy density and power densities of the supercapacitors were calculated using Eqs. (2) and (3) respectively:

$$C_m = \frac{I \cdot \Delta t}{\Delta V \cdot m} \quad (1)$$

$$E = \frac{1}{2} C_m \cdot \Delta V^2 \quad (2)$$

$$P = \frac{E}{\Delta t} \quad (3)$$

where C$_m$ (F g^{-1}) is the mass specific capacitance, m (g) is the mass of active materials in the electrode, I (A) is response current, Δt (s) is discharge time, ΔV (V) is potential windows of the discharge process (excluding the IR drop), E is the specific energy density (Wh kg^{-1}), P is power density (kW kg^{-1}).

Figure 5b shows the cyclic voltammetry (CV) curves of the supercapacitor at different scan rates with the potential window ranging from 0 to 0.8 V. The approximate rectangular shapes with large enclosed area of the CV curves indicate the flexible device with a good performance. The absence of redox peaks for the CV curves indicate that the electrode charge and discharge at a pseudo-constant rate over the entire CV process. The CV curves of the devices under flat and bent conditions are essentially the same (Fig. 6b), demonstrating its excellent electrical stability and flexible electrochemical behavior. The GCD curves of the supercapacitor are tested at different current density (Fig. 5c). An ideal supercapacitor usually exhibit the symmetrical triangle shapes and small IR drop, revealing that the redox reaction is reversible (Peng et al. 2017). The IR drop is usually caused by the overall internal resistance of the devices. The lower internal resistance of the devices indicates less energy waste. Figure 5c shows that the GCD curves are almost symmetrical at different current density and there was a small IR drop, indicating that the supercapacitor has better capacitive property. The C$_m$ value of the devices is 206.8 F g^{-1} at a current density of 1 mA cm^{-2}.

Nyquist plot (Fig. 5d) was obtained for flat and bent supercapacitors. In the circuit, R$_s$ is regarded as a series of resistances including the intrinsic resistance of the electrode, the ionic resistance of the bulk electrolyte, and the interface resistance at the electrode/electrolyte and electro/current collector. C represents the double-layer capacitance; CPE stands for Faradic pseudocapacitance caused by electrochemical surface reactions. R$_{ct}$ is the charge transfer resistance, arising from Faradic reaction and electronic double-layer capacitor at the interface between the electrode and electrolyte. Z$_w$ is the Warburg impedance originated from the frequency dependence of ion diffusion/transport in the surface of electrolyte/electrode (Li et al. 2017). The measured impedance spectra were
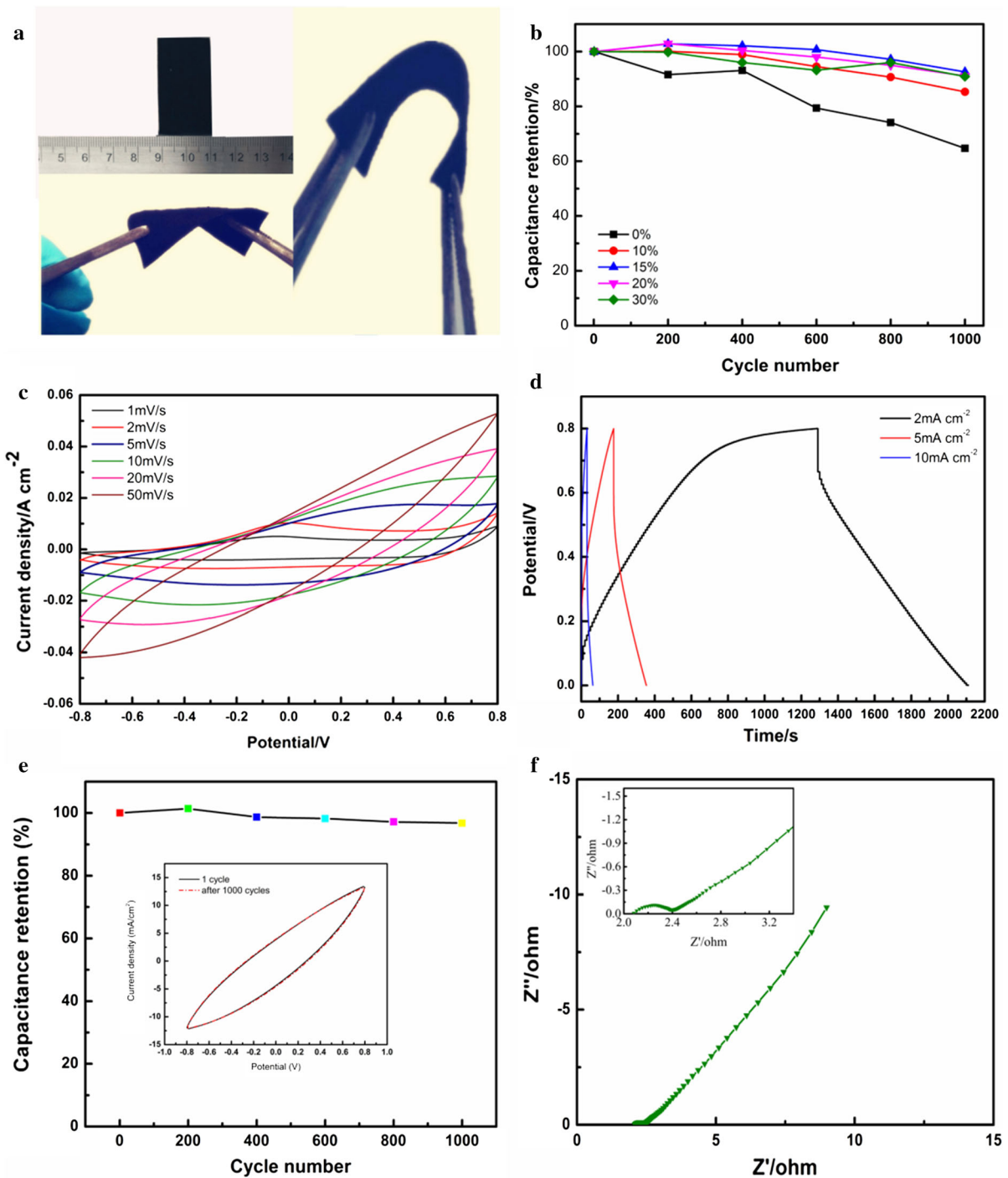
Fig. 4 a Sheet resistances of the electrodes prepared under different mass of MWCNT, **b** capacitance retention of the electrodes prepared with different MWCNT content, **c**, **d** the CV and GCD curves of the cotton/PPy/MWCNT electrode, **e** cycling stability of the synthesis electrode, **f** Nyquist plots of cotton/PPy/MWCNT electrode

analyzed by ZSimpWin software on the basis of the equivalent circuit (Fig. 5d), in which the equivalent

series resistance (R_s) value was 13.3 Ω and the charge transfer resistance (R_{ct}) was 1.7 Ω. Furthermore, the
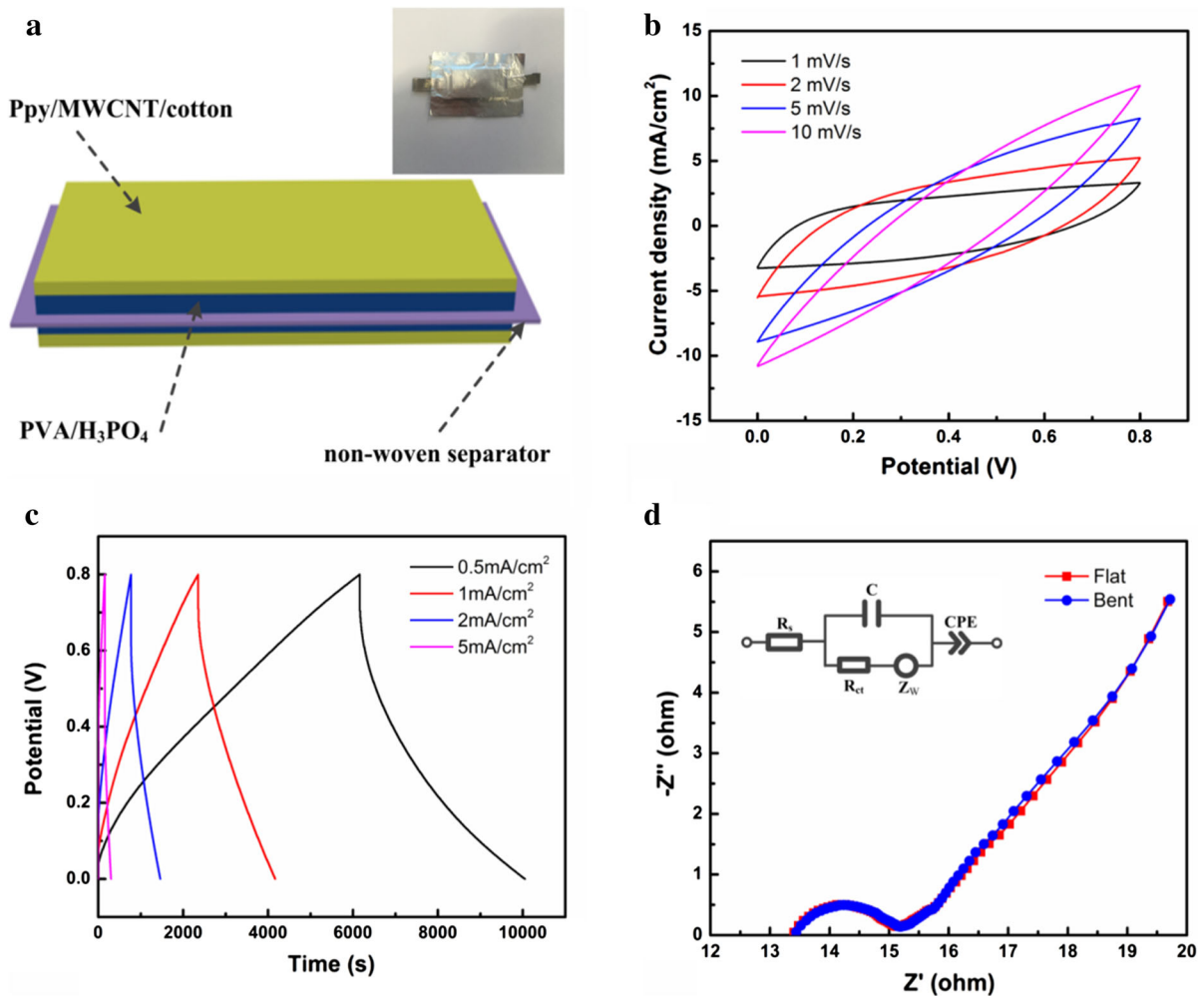
Fig. 5 a Schematic diagram and photograph of the supercapacitor, **b** CV curves of the supercapacitor at different scan rate, **c** GCD curves of the supercapacitor at different current density, **d** Nyquist plots the supercapacitor at flat and bent at an angle of 90°, the insert shows the equivalent circuit of the assembled supercapacitor at flat and bent

Nyquist plot under flat and bent at an angle of 90° was also similar (Fig. 5c), illustrating the excellent flexible performance.

The leakage current is one of the most significant problems in supercapacitors and the low leakage current the device make practical applications promising (Adu et al. 2017; Saravanakumar et al. 2017). We have measured the parameter for our device with the results presented in Fig. 6a. The leakage current was measured by applying a device full potential and measured a current required for maintaining that potential. Figure 6a shows the leakage current, in which current drops abruptly from 0.013 to 0.005 mA at the initial stage and after being stabilised at

0.004 mA over a time period of more than 2 h when held at 0.8 V.

The C_m values for the devices at different current density are shown in Fig. 6c. It can be found that the C_m values decreased with the increase of the current densities and the capacitance of the device is 41.54% retained when the current density increases from 0.5 to 5 mA cm^{-2}. The Ragon plots of the supercapacitor are shown in Fig. 6d. Accordingly, the power density of the device can reach to about 201 W kg^{-1}, and the energy density can reach about 19.6 Wh kg^{-1}. In addition, the device retains about 72% of the initial capacitance after 400 charge–discharge cycles at a current density of 3 mA cm^{-2} (Fig. 6e). At the same
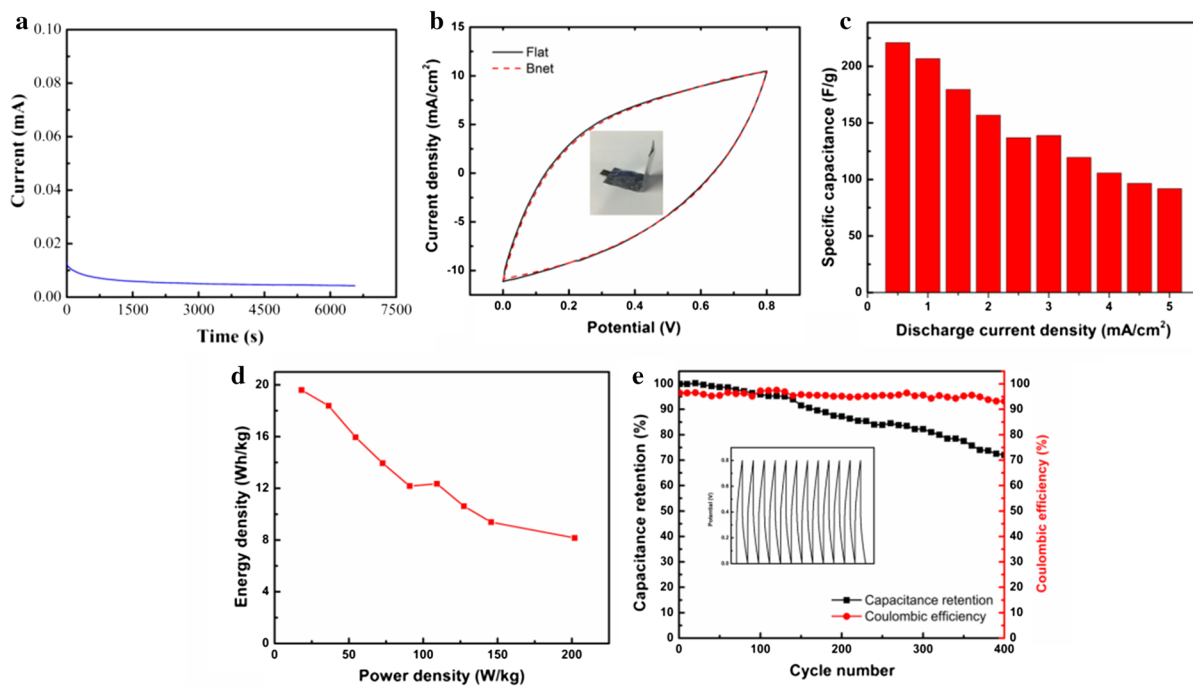
Fig. 6 **a** The leakage current curves of the supercapacitor, **b** cyclic voltammograms of the supercapacitor at 2 mV s^{-1} under flat and bent, **c** specific capacitances at different current density, **d** Ragon plots of the supercapacitor, **e** capacitance retention and coulombic efficiency of supercapacitor at an angle of 90°. The insert displays the GCD curve of supercapacitor for the last 12 cycles

time, the associated coulombic efficiency retains about 95% charge during the charge–discharge cycle process. The charge–discharge curve for the last 12 cycles further confirms its long cycle stability and good electrochemical reproducibility (Fig. 6e).

Conclusion

In summary, flexible cotton/PPy/MWCNT electrodes were synthesized using a simple one-pot polymerization process. The obtained electrode had a three-dimensional structure with a high capacitance of 597 F g^{-1} at a scan rate of 1 mV s^{-1} and high capacitance retention (96.8%) after 1000 cycles, when the mass of MWCNT relative to PPy was 20%, and the concentration of SDBS and TsOH were 0.05 and 0.15 M respectively. In addition, a flexible all solid-state supercapacitor based on the synthesized cotton/PPy/MWCNT electrodes was fabricated. These electrodes were flexible enough to be twisted and bent without obvious capacitance loss. The fabricated device has a high capacitance of 206.8 F g^{-1} at a

current density of 1 mA cm^{-2} and high capacitance retention of 72% after 400 charge–discharge cycles when bent at an angle of 90°. This study showed a promising potential for simple fabrication of flexible, cost-effective, and high-performance supercapacitors, providing a new pathway for the fabrication of various power-wearable electronics.

References

Adu K, Ma D, Wang Y, Spencer M, Rajagopalan R, Wang CY, Randall C (2017) Flexible robust binder-free carbon nanotube membranes for solid state and microcapacitor application. Nanotechnology 29:035606–035607

Bao L, Li X (2012) Towards textile energy storage from cotton T-shirts. Adv Mater 24:3246–3252

Beidaghi M, Gogotsi Y (2014) Capacitive energy storage in micro-scale devices: recent advances in design and fabrication of micro-supercapacitors. Energy Environ Sci 7:867–884

Biniak S, Dzieleńdziak B, Siedlewski J (1995) The electrochemical behaviour of carbon fibre electrodes in various electrolytes. Double-layer capacitance. Carbon 33:1255–1263

Borenstein A, Hanna O, Ran A, Luski S, Brousse T, Aurbach D (2017) Carbon-based composite materials for supercapacitor electrodes: a review. J Mater Chem A 5:12653–12672

Cai J et al (2015) High-performance supercapacitor electrode materials from cellulose-derived carbon nanofibers. ACS Appl Mater Interfaces 7:14946–14953

Firoz BK, Siva Subramanian SP, Anbu KM (2013) Functionalisation of fabrics with conducting polymer for tuning capacitance and fabrication of supercapacitor. Carbohydr Polym 94:487–495

Ford ENJ, Mendon SK, Thames SF, Ph D, Rawlins JW, Ph D (2010) X-ray diffraction of cotton treated with neutralized vegetable oil-based macromolecular crosslinkers. J Eng Fibers Fabr 5:10–20

Gao Y (2017) Graphene and polymer composites for supercapacitor applications: a review. Nanoscale Res Lett 12:387–404

Ge D, Yang L, Fan L, Zhang C, Xiao X, Gogotsi Y, Yang S (2015) Foldable supercapacitors from triple networks of macroporous cellulose fibers, single-walled carbon nanotubes and polyaniline nanoribbons. Nano Energy 11:568–578

Hu L, Cui Y (2012) Energy and environmental nanotechnology in conductive paper and textiles. Energy Environ Sci 5:6423–6435

Hu L, Pasta M, Mantia FL, Cui LF, Jeong S, Deshazer HD, Choi JW, Han SM, Cui Y (2010) Stretchable, porous, and conductive energy textiles. Nano Lett 10:708–714

Huang S, Chen P, Lin W, Lv S, Chen G, Yin X, Chen W (2016) Electrodeposition of polypyrrole on carbon nanotube-coated cotton fabrics for all-solid flexible supercapacitor electrodes. Rsc Adv 6:13359–13364

Jagadale AD, Guan G, Du X, Hao X, Li X, Abudula A (2015) Cobalt hydroxide [Co(OH)$_2$] loaded carbon fiber flexible electrode for high performance supercapacitor. Rsc Adv 5:56942–56948

Kang ET, Neoh KG, Ong YK, Tan KL, Tan BTG (1991) X-ray photoelectron spectroscopic studies of polypyrrole synthesized with oxidative Fe(III) salts. Macromolecules 24:2822–2828

Karim MR, Lee CJ, Chowdhury AMS, Nahar N, Mu SL (2007) Radiolytic synthesis of conducting polypyrrole/carbon nanotube composites. Mater Lett 61:1688–1692

Kim JY, Kim KH, Kim KB (2008) Fabrication and electrochemical properties of carbon nanotube/polypyrrole composite film electrodes with controlled pore size. J Power Sources 176:396–402

Lee SY, Kim JI, Park SJ (2014) Activated carbon nanotubes/polyaniline composites as supercapacitor electrodes. Energy 78:298–303

Li L, Seng KH, Liu H, Nevirkovets IP, Guo Z (2013a) Synthesis of Mn$_3$O$_4$-anchored graphene sheet nanocomposites via a facile, fast microwave hydrothermal method and their supercapacitive behavior. Electrochim Acta 87:801–808

Li S, Guo Z, Wang C, Wallace G, Liu H (2013b) Flexible cellulose based polypyrrole-multiwalled carbon nanotube films for bio-compatible zinc batteries activated by simulated body fluids. J Mater Chem A 1:14300–14305

Li Y, Wang G, Wei T, Fan Z, Yan P (2016) Nitrogen and sulfur co-doped porous carbon nanosheets derived from willow catkin for supercapacitors. Nano Energy 19:165–175

Li X, Zhou M, Wang J, Ge F, Zhao Y, Komarneni S, Cai Z (2017) Flexible and internal series-connected supercapacitors with high working voltage using ultralight porous carbon nanofilms. J Power Sources 342:762–771

Liu C, Yu Z, Neff D, Zhamu A, Jang BZ (2010) Graphene-based supercapacitor with an ultrahigh energy density. Nano Lett 10:4863–4868

Liu WW, Yan XB, Lang JW, Peng C, Xue QJ (2012) Flexible and conductive nanocomposite electrode based on graphene sheets and cotton cloth for supercapacitor. J Mater Chem 22:17245–17253

Liu L, Niu Z, Zhang L, Zhou W, Chen X, Xie S (2014) Nanostructured graphene composite papers for highly flexible and foldable supercapacitors. Adv Mater 26:4855–4862

Liu C, Cai Z, Zhao Y, Zhao H, Ge F (2015) Potentiostatically synthesized flexible polypyrrole/multi-wall carbon nanotube/cotton fabric electrodes for supercapacitors. Cellulose 23:637–648

Liu C, Cai Z, Zhao Y, Zhao H, Ge F (2016) Potentiostatically synthesized flexible polypyrrole/multi-wall carbon nanotube/cotton fabric electrodes for supercapacitors. Cellulose 23:637–648

Miller JR, Outlaw RA, Holloway BC (2011) Graphene electric double layer capacitor with ultra-high-power performance. Electrochim Acta 56:10443–10449

Nyström G, Razaq A, Strømme M, Nyholm L, Mihranyan A (2009) Ultrafast all-polymer paper-based batteries. Nano Lett 9:3635–3639

Peng S, Fan L, Wei C, Liu X, Zhang H, Xu W, Xu J (2017) Flexible polypyrrole/copper sulfide/bacterial cellulose nanofibrous composite membranes as supercapacitor electrodes. Carbohydr Polym 157:344–352

Qian T, Yu C, Wu S, Shen J (2013) A facilely prepared polypyrrole–reduced graphene oxide composite with a crumpled surface for high performance supercapacitor electrodes. J Mater Chem A 1:6539–6542

Saravanakumar B, Jayaseelan SS, Seo MK, Kim HY, Kim BS (2017) NiCo$_2$S$_4$ nanosheet-decorated 3D, porous Ni film@Ni wire electrode materials for all solid-state asymmetric supercapacitor applications. Nanoscale 9:18819–18834

Sawangphruk M, Srimuk P, Chiochan P, Krittayavathananon A, Luanwuthi S, Limtrakul J (2013) High-performance supercapacitor of manganese oxide/reduced graphene oxide nanocomposite coated on flexible carbon fiber paper. Carbon 60:109–116

Shi K, Zhitomirsky I (2013) Fabrication of polypyrrole-coated carbon nanotubes using oxidant-surfactant nanocrystals for supercapacitor electrodes with high mass loading and enhanced performance. ACS Appl Mater Interfaces 5:13161–13170

Song Y, Li Z, Guo K, Shao T (2016) Hierarchically ordered mesoporous carbon/graphene composites as supercapacitor electrode materials. Nanoscale 8:15671–15680

Stoller MD, Park S, Zhu Y, An J, Ruoff RS (2008) Graphene-based ultracapacitors. Nano Lett 8:3498

Tamm J, Raudsepp T, Marandi M, Tamm T (2007) Electrochemical properties of the polypyrrole films doped with benzenesulfonate. Synth Met 157:66–73

Tang Q, Chen M, Yang C, Wang W, Bao H, Wang G (2015) Enhancing the energy density of asymmetric stretchable supercapacitor based on wrinkled CNT@MnO$_2$ cathode and CNT@polypyrrole anode. ACS Appl Mater Interfaces 7:15303–15313

Wang PC, Yu JY (2012) Dopant-dependent variation in the distribution of polarons and bipolarons as charge-carriers in polypyrrole thin films synthesized by oxidative chemical polymerization. React Funct Polym 72:311–316

Wang YG, Cheng L, Xia YY (2006) Electrochemical profile of nano-particle CoAl double hydroxide/active carbon supercapacitor using KOH electrolyte solution. J Power Sources 153:191–196

Wang S, Pei B, Zhao X, Dryfe RAW (2013) Highly porous graphene on carbon cloth as advanced electrodes for flexible all-solid-state supercapacitors. Nano Energy 2:530–536

Wang K, Wu H, Meng Y, Wei Z (2014) Conducting polymer nanowire arrays for high performance supercapacitors. Small 10:14–31

Xie B et al (2015) Shape-tailorable graphene-based ultra-high-rate supercapacitor for wearable electronics. ACS Nano 9:5636–5645

Xiong Z, Liao C, Han W, Wang X (2015) Mechanically tough large-area hierarchical porous graphene films for high-performance flexible supercapacitor applications. Adv Mater 27:4469–4475

Xu J et al (2015a) Fabric electrodes coated with polypyrrole nanorods for flexible supercapacitor application prepared via a reactive self-degraded template. Org Electron 26:292–299

Xu J et al (2015b) Polypyrrole/reduced graphene oxide coated fabric electrodes for supercapacitor application. Org Electron 24:153–159

Xu J et al (2015c) Polypyrrole-coated cotton fabrics for flexible supercapacitor electrodes prepared using CuO nanoparticles as template. Cellulose 22:1355–1363

Xue J (2013) An all-cotton-derived, arbitrarily foldable, high-rate, electrochemical supercapacitor. Phys Chem Chem Phys 15:8042–8045

Yang P et al (2014) Reciprocal alternate deposition strategy using metal oxide/carbon nanotube for positive and negative electrodes of high-performance supercapacitors. Nano Energy 10:108–116

Yesi Y, Shown I, Ganguly A, Ngo TT, Chen LC, Chen KH (2016) Directly-grown hierarchical carbon nanotube@polypyrrole core-shell hybrid for high-performance flexible supercapacitors. Chemsuschem 9:370–378

Zhang B et al (2011) A facile synthesis of polypyrrole/carbon nanotube composites with ultrathin uniform and thickness-tunable polypyrrole shells. Nanoscale Res Lett 6:431–440